PCCP



PAPER View Article Online
View Journal | View Issue



Cite this: *Phys. Chem. Chem. Phys.*, 2023, **25**, 17943

Received 11th April 2023, Accepted 8th June 2023

DOI: 10.1039/d3cp01655b

rsc.li/pccp

GFP-related chromophores: photoisomerization, thermal reversion, and DNA labelling†

Martin S. Faillace, ^{ab} Ekaterina A. Dolgopolova, ^b Noelia M. Ceballos, ^{ba} E. Nahir Ruiz Pereyra, ^a Lucia Lanfri, ^a Gustavo A. Argüello, ^a Maximiliano Burgos Paci, ^a Natalia B. Shustova ^{bb} and Walter J. Peláez ^{b*}

Due to the pronounced effect of the confined environment on the photochemical properties of 4-hydroxybenzylidene imidazolinone (HBI), a GFP-related chromophore, imidazolidinone and imidazothiazolone analogues have been studied as fluorescent probes. Their photoisomerization and their thermal reversion were studied under 365-nm-irradiation, resulting in observation of an enthalpy-entropy compensation effect. Theoretical studies were carried out to shed light on the thermal reversion mechanism. Moreover, photophysical studies of benzylidene imidazothiazolone in the presence of dsDNA revealed fluorescence enhancement. The prepared compounds could be considered as a valuable tool for the detailed investigation of physicochemical, biochemical, or biological systems.

Introduction

Green fluorescent protein (GFP) is an imaging tool broadly used in molecular biology and in medicine to visualize various biological events. The chromophore of the GFP, 4-hydroxybenzylidene imidazolinone (HBI), can isomerize from Z to E. It is well known that the Z isomer acts as an efficient fluorophore, while the E configuration possesses an extremely weak fluorescence. This particular behaviour is also strongly dependent on the environment that the scaffold of the protein senses, defining chromophore photophysics. For this reason, several studies with HBI analogues have been carried out and promoted the importance of the subject. $^{3-6}$

From a different perspective, there are many studies focused on the biological activities of 5-arylmethylene imidazolidinones. For instance, it was found that a combination of the thiocarbonyl group and C5 benzylidene substituent could be a recognition motif for P450 metabolism in a human hepatocyte model. Our recent findings demonstrated the antioxidant properties as well as the modulatory activity of some imidazolidinone derivatives, along with a noteworthy light-enhanced activity against *S. aureus*. ^{10,11} That is, some imidazolidinone compounds were able to inhibit the growth of *S. aureus* ATCC 25923 upon UV irradiation. This last result reinforces the need

Moreover, a fundamental understanding of the interaction of DNA with small organic molecules is crucial for the development of new drugs for cancer treatment as well as addressing overcoming bacterial resistance to antibiotics. ^{12,13} There are examples of this core in different applications, ¹⁴ for instance, DNA labelling, ^{14–16} which can be studied using emission techniques.

In our previous work, we demonstrated the experimental and theoretical evidence for photoisomerization and thermal reversion of 5-arylmethylene-2-thioxoimidazolidin-4-one. Herein, we expanded the scope of the considered derivatives using a number of different aryl substituents, among which there are some compounds with promising biological activities as mentioned above. Furthermore, to introduce a structural change, the sulfur atom was used to build a bicyclic moiety as shown in Scheme 1. As previously described, the environment of the HBI chromophore plays a crucial role in its photophysics, encouraging us to provide deeper insights into the fluorescence properties of the heterocycles in the presence of dsDNA. Notably, these heterocycles have functional moieties for hydrogen bonding,

Scheme 1 Photoisomerization $Z \rightarrow E$ and thermal reversion $E \rightarrow Z$.

for understanding the photochemical features of these heterocyclic compounds from a molecular point of view.

^a INFIQC-CONICET-Dpto. de Fisicoquímica, Facultad de Ciencias Químicas, Universidad Nacional de Córdoba, Ciudad Universitaria, Córdoba, X5000HUA, Argentina. E-mail: walter.pelaez@unc.edu.ar

b Department of Chemistry and Biochemistry, University of South Carolina, Columbia, South Carolina 29208, USA

[†] Electronic supplementary information (ESI) available. See DOI: https://doi.org/10.1039/d3cp01655b

suitable for interacting with DNA. As an outcome, we believe that this work contributes to the fundamental understanding of the photochemical properties of the HBI-related arylmethylene heterocycles.

Experimental section

Synthesis of imidazolidines and imidazothiazolones (**1a-c** and **2a-c**) were performed by microwave irradiation in a monowave 300 Anton Paar, based on previously described conventional methodologies. ^{10,18} Imidazolidines **1a-c** were purified by column chromatography (CHCl₃:EtOH, 90:10) while imidazothiazolones **2a-c** were purified by preparative Thin-Layer Chromatography (CH₂Cl₂:EtOAc, 80:20). All compounds were characterized using spectroscopic techniques including NMR (1D- & 2D) and UV-vis spectroscopy as well as mass spectrometry; all acquired data are in agreement with the proposed structures.

UV-vis spectra of chromophores in acetonitrile (HPLC grade) were recorded on a UV-1601 Shimadzu spectrophotometer using a quartz cell with an optical path length of 1-cm.

The reaction yields for the compounds **2a–c** were determined by HPLC. Elution was performed with a mixture of CH₃OH:H₂O (90:10) at a flow rate of 0.8 mL min⁻¹. The experiments were performed employing a Waters 1525 Binary Pump connected to a Waters 2998 Photodiode Array Detector, and a C18 column (5 μ m \times 4.5 μ m \times 15 cm).

For characterization of the compounds, NMR spectra were recorded in DMSO- d_6 and acetone- d_6 on a Bruker Avance II 400 MHz spectrometer (BBI probe, z gradient) (1 H at 400.16 MHz, 13 C at 100.56 MHz and 19 F at 376.53 MHz) at 22 $^{\circ}$ C. Chemical shifts are reported in parts per million (ppm) downfield from TMS.

Gas chromatography/mass spectrometry (GC/MS) analyses were performed on a Shimadzu GC-MS-QP 5050 spectrometer equipped with a VF column (30 m \times 0.25 mm \times 5 μ m) using helium as the eluent at a flow rate of 1.1 mL min⁻¹. The injector and ion source temperature were 280 °C, the pressure in the MS instrument was 10⁻⁵ Torr, and MS recordings were made in the electron impact mode (EI) at an ionization energy of 70 eV.

The photoisomerization and the thermal reversion were monitored by the integration of the $^1\mathrm{H}$ NMR spectra between 45–75 $^\circ\mathrm{C}$. For this purpose, a Bruker Avance III-HD 300 MHz spectrometer was used. A 365-nm LED lamp (M365L2, Thorlabs) was used as an excitation source. The corresponding solutions were prepared in CD₃CN.

To investigate the electronic structure and potential energy surfaces of 1a–c and 2a–c, we used *ab initio* quantum chemistry. No symmetry constraints were imposed neither on molecular geometries nor electronic wave functions. Optimization and vibrational frequencies of the ground state geometries were performed at the B3LYP/6-311+g(d,p) level. To confirm the transition state structures, frequency and intrinsic reaction coordinate (IRC) calculations were performed.

The complete active space–self-consistent field (CASSCF) method was used to obtain the excited electronic state (T_1) .

This method is described by the number of states included in the average (N) and the number of electrons (n) and orbitals (m) included in the active space. The five orbitals that constitute the active space are the HOMO-2, HOMO-1, HOMO, LUMO, and LUMO+1, as previously described. ¹⁷ All stationary potential energy points, including electronic state minima and degeneracies, were optimized with the SA-2-CAS(6/5) method. The 6-31G(d) basis set was used for all CASSCF calculations.

Time-dependent density functional theory (TD-DFT/6-311+g(d,p)) was used to model the energies and properties of the electronically excited states. We have included solvent contributions using the PCM solvent model at S_0 and T_1 . All calculations were performed with Gaussian 09.¹⁹

The fluorescent profile was examined in the absence and presence of fish dsDNA (0.029%P/P). DNA solutions were prepared in TE buffer (Tris 10 mM, EDTA 1 mM, pH 7.5). The sample solutions were initially diluted in DMSO, rising to a final concentration of 0.3 mM in the cuvette (16%V/V DMSO). A solution of ethidium bromide (EtBr) at 15 μ M was used as a positive control. All the analyses were performed at a controlled temperature (30 °C). Fluorescence spectra were measured using a PTI QM2 (Quanta Master 2) spectrofluorometer from Photon Technology International which utilizes a pulsed Xe lamp (75 W) as the excitation source and a photon-counting detector. An excitation wavelength of 307 nm was used, and the fluorescence spectra were recorded in the range from 350 to 750 nm.

Results and discussion

Synthesis

A series of HBI-related analogues were prepared using microwave synthesis as shown in Scheme 2. As described in our previous work, 5-arylmethylene thioxoimidazolidinones (1a-c) were prepared through the condensation reaction of thiohydantoin with different aromatic aldehydes (path A), in 69–96% yields. The 5-arylmethylene imidazothiazolone derivatives were prepared using two different synthetic approaches. The first approach for the synthesis of imidazothiazolones (2a-c) was based on the reaction of (1a-c) with 1,2-dichloroethane. However, this synthetic route had some limitations due to hydrolysis of the desired product. Efforts to improve the

Scheme 2 Synthesis of arylidene thioxoimidazolidinones (1a-c) and imidazothiazolones (2a-c) derivatives.

PCCP Paper

synthetic procedure (see the ESI† for more details) led to the second approach which includes the one-pot synthesis described in Scheme 2 (path B), that turned out to be an efficient procedure to prepare benzylidene imidazothiazolone derivatives (e.g., compound 2a, 98% yield).

The formation of 2a could be postulated considering two different pathways. It is known that thiohydantoin is in equilibrium with the thiol tautomer^{20,21}; for this reason, the nucleophilic attack to the alkyl group could be initiated either by the thiol group or the nitrogen lone pair of the thiohydantoin. To address this question, a reaction of 1-bromoethane with 1a was performed. As shown in Scheme 3, if the reaction occurred via the nitrogen, compound 3 should be detected, while compound 4 would be identified if the nucleophilic attack occurred via the sulphur atom. After completion of the reaction, compound 4 resulted as the main product of the reaction. Additionally, a sub-product that incorporated two ethyl groups was also detected (5). These compounds were elucidated by ¹H-NMR spectroscopy and GC/MS, as shown in Fig. S1 and S2 in the ESI.†

Photoisomerization and thermal reversion

Our heterocyclic compounds (1a-c and 2a-c) were almost exclusively in the Z form. In addition, they presented similar strong absorption bands between 340 and 380 nm, as shown in section 4 of the ESI.† In a previous publication, we demonstrated that photoisomerization of 1a is a monophotonic process occurring through the rotation of the dihedral angle (τ) in a biradical pathway.¹⁷ In this work, we explored the photochemical behaviour of other derivatives, with different substituents on the phenyl group: one electron-donating group by the inductive effect (1b) and an electron-withdrawing substituent (1c). Moreover, compounds 2a-c were designed with the purpose of re-functionalizing the heterocyclic moiety, leading to the more planar structures, which favour their interaction with DNA.16

Solutions of arylidene heterocycles were prepared in CD₃CN due to the high viscosity of DMSO- d_6 , which drastically increased their thermal reversion times. The isomerization and thermal reversion (Scheme 1) was monitored by ¹H NMR spectroscopy following the signal of the vinyl hydrogen. The concentration of each isomer was calculated by integration of ¹H NMR spectra at different irradiation times. The samples were isomerized using a 365-LED lamp leading to the increase of the E isomer concentration with time until a photostationary state (PSS) is achieved as shown in Fig. 1.

At 25 °C, only compounds 1a and 1c have a measurable concentration of the E isomer, since the methylated derivative 1b and all the bicyclic compounds (2a-c) have the Z conformation exclusively. Regarding compound 1b, its conformation can be attributed to the size of the methyl substituent and its solvent box, which precludes isomerization at room temperature. Moreover, our findings are in line with the observations for 5-arylmethylenehydantoins studied by Tan et al., 22 who suggested that the Z/E equilibrium ratio is higher with the electron-donating groups on the benzene ring.22

Interestingly, compounds 1a-c reached the PSS, with a higher concentration of the Z isomer. In contrast to the fused imidazothiazolone (2a-c), for which the concentration of the Eisomer predominates (Table 1).

Once the PSS was achieved, and after stopping the irradiation, the E-isomers were thermally isomerized to the Z conformation in a unimolecular process. 17 This process was very slow and despite our attempts to advance isomerization with acetic acid, either in DMSO-d₆ or CD₃CN, no net effect was observed. Moreover, the samples after reaching the PSS were irradiated at 590 nm to induce the photo-reversion reaction as it was previously reported by Tan et al on 5-arylmethylenehydantoin²³; but after 50 min of irradiation, no changes in the concentration of either isomers were detected.

Thermal $E \to Z$ isomerization of compounds 1a-c and 2a-c (Scheme 3) was investigated as a function of temperature (from 45 to 75 °C) in CD₃CN. An example of the thermal reversion progress is shown for compound 2a at 45 and 75 °C (Fig. 2). The complete set of exponential decays is detailed in the ESI.† The Arrhenius plots for the studied compounds are shown in Fig. 3. The use of the Eyring equation gave a complete determination of the activation parameters which are detailed in Table 2. The equations used to determine the physicochemical parameters are presented in the ESI† (page S17).

The process "photoisomerization-thermal reversion" was repeated for several cycles without apparent decomposition of the studied compounds, meaning that both isomers are thermally (45-75 °C) as well as photochemically (under 365-nm irradiation) stable.

The evaluated isomerization rate constant (k) of the bicyclic compounds (2a-c) is 1.3 to 3-fold higher than that calculated for thioxoimidazolidinones 1a-c. Previous reports for GFPchromophore analogues mention that an electron-withdrawing group at the phenyl moiety accelerates the thermal isomerization when the addition/elimination mechanism takes place. 24,25

Scheme 3 Experimental mechanistic study in the formation of 2a.

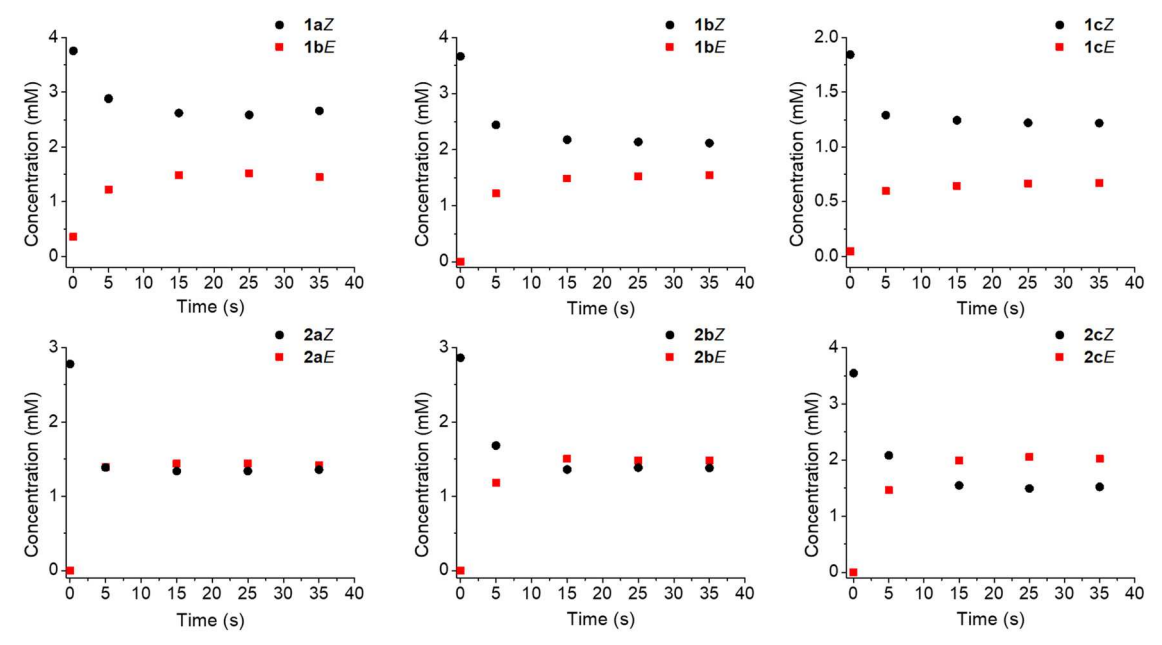


Fig. 1 Formation of E isomer and Z consumption until achieving the photostationary state of the thioxoimidazolidinones and imidazothiazolones compounds 1a-c and 2a-c.

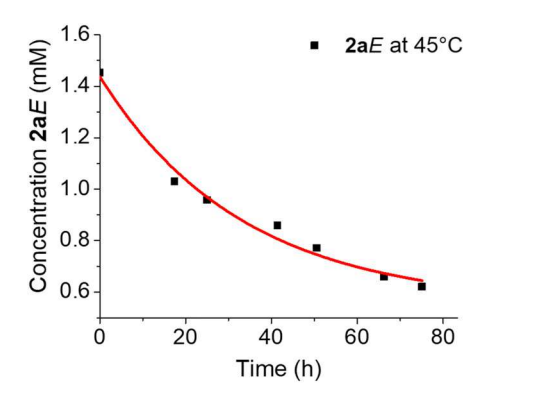
Table 1 Thermal equilibrium and photostationary state population of Z/E isomers

	Thermal equilibrium	Photostationary state	$\log(\varepsilon)$	
Compounds	Z:E (%)	Z:E (%)		
1a	91:9	65:35	4.25	
1b	100:0	58:42	4.55	
1c	98:2	65:35	4.49	
2a	100:0	49:51	4.31	
2b	100:0	48:52	4.45	
2c	100:0	43:57	4.97	

However, in our findings, the isomerization rates of the compounds with a fluorine substituent (1c and 2c) are lower than those of the other derivatives. This result is congruent with our previous result where the mechanism operating is through a diradical pathway.17

At the same time, the Van't Hoff plot in Fig. 4 denotes the lack of an intersection point, which emphasizes that there is not an isokinetic effect, as can be expected due to the differences in the isomerization rates shown in Table 2. For this reason, it is challenging to evaluate the thermodynamic enthalpy of these processes. Nevertheless, as indicated in Table 2, the free energies of activation are very similar, and consequently, a compensation effect was observed in the enthalpy-entropy correlation plot, as shown in Fig. 4. The correlation coefficient of the linear plot (0.9998) can be used as a criterion for this assumption.²⁶

Theoretical calculations. As previously proposed for compound 1a, thermal isomerization from E to Z species would be accomplished through the formation of a biradical intermediate via an S₀-T₁ intersystem crossing (ISC) which is less energetic than simple twisting.¹⁷ In this work, we performed further calculations in both the gas phase and solution, where the polarizable conductor calculation model of solvation (CPCM)



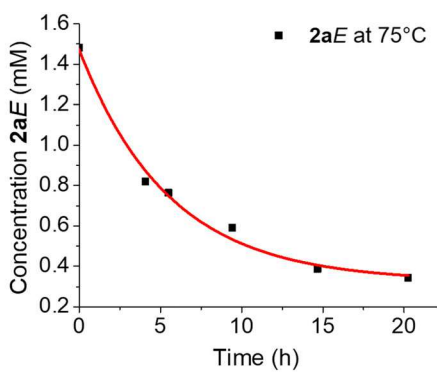
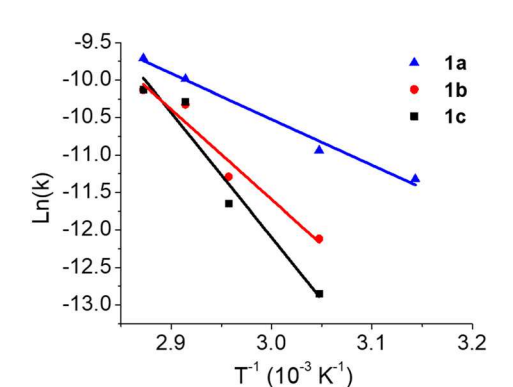


Fig. 2 Temporary exponential decay of the 2aE isomer at two temperatures, (left) 45 and (right) 75 °C.

PCCP



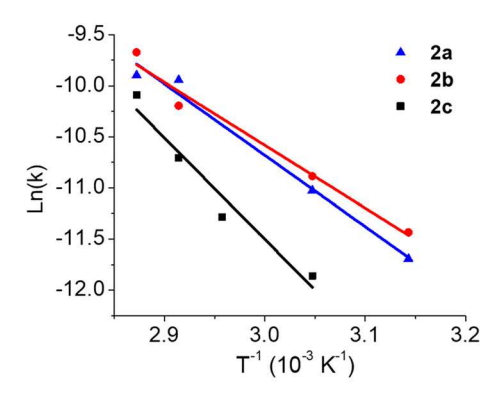
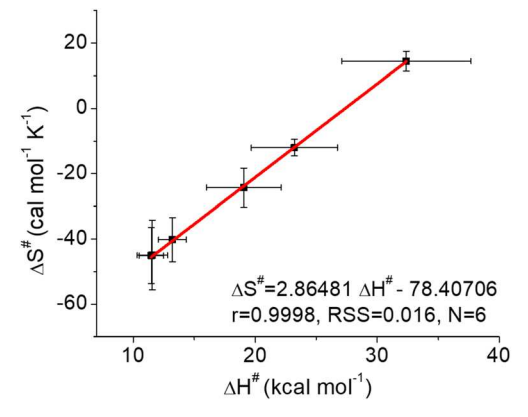


Fig. 3 Arrhenius plot for all analyzed compounds.

Table 2 Kinetic and activation parameters for $E \rightarrow Z$ thermal isomerization

Compounds	$k (10^{-5} \text{ s}^{-1})$	log(A)	$\Delta S^{\#}$ (cal K ⁻¹ mol ⁻¹)	Ea (kcal mol ⁻¹)	$\Delta H^{\#a}$ (kcal mol ⁻¹)	$\Delta G^{\#a}$ (kcal mol ⁻¹)
1a	1.3	3.4	-45.0	12.2	11.5	26.9
1b	1.3	10.6	-11.9	23.9	23.2	27.3
1c	0.9	16.4	14.6	33.1	32.4	27.4
2a	1.7	4.5	-40.1	13.9	13.2	27.0
2b	3.7	3.4	-44.9	12.2	11.6	26.9
2c	1.3	7.9	-24.2	19.7	19.1	27.4



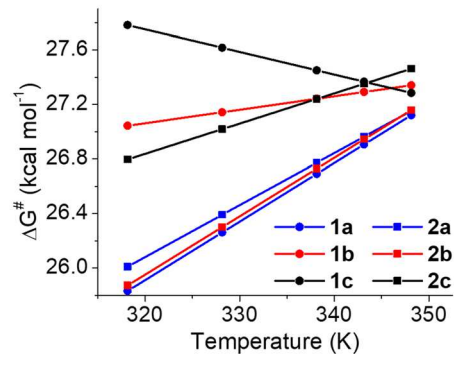


Fig. 4 Enthalpy-entropy compensation plot (left) and Van't Hoff plot (right).

was used to extend our assumption to the whole set of compounds.

Ground state B3LYP/6-311+g(d,p) gas-phase calculations show that Z isomers of **1a–c** and **2a–c** are more stable than their E counterparts by approximately 2–4 kcal mol^{-1} . Moreover, the gas-phase barrier for $E \to Z$ conversion through simple dihedral rotation is about 63–75 kcal mol^{-1} and 48–71 kcal mol^{-1} **1a–c** and **2a–c**, respectively (Table 3).

To achieve a better fit of the theoretical values with the experimental ones, we have performed CPCM calculations (in acetonitrile as a solvent) implemented in Gaussian. This particular solvent was chosen because thermal reactions, monitored by the NMR spectroscopy, were also performed in acetonitrile- d_3 . In this case, the calculated values of the energy

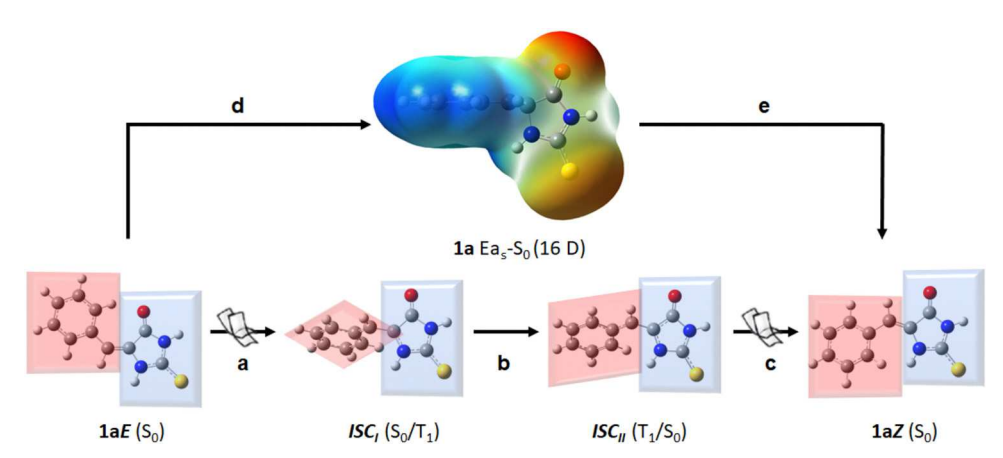
barrier for the isomerization E–Z are lower in energy than those obtained in the gas phase. For instance, for compounds $\mathbf{1a}$ – \mathbf{c} the energy barriers in acetonitrile are almost 10 kcal mol^{-1} lower in comparison with the gas phase values while for the cycled compounds ($\mathbf{2a}$ – \mathbf{c}) they are almost 5 kcal mol^{-1} more stable in solution than in gas phase (Table 3). In all cases, a twisted conformation corresponds to the transition state, which is characterized by its zwitterionic nature. Therefore, the potential energy surfaces in solution (PESs, S_0 and T_1) were calculated for all compounds studied herein. These calculations are weight evidence on the reaction pathway proposed in our previous article for $\mathbf{1a}$, 17 via a biradical species (Scheme 4, paths \mathbf{a} – \mathbf{c}), which is lower in energy compared to the simple twisting of the double bond of the benzylidene moiety for all

PCCP Paper

Table 3 Energetic and thermodynamic parameters calculated by using Gaussian09 (B3LYP/6-311+q(d,p))^{ab}

Compound	Gas phase (S ₀)		Acetonitrile solution (S ₀)		Acetonitrile solution (T ₁)			Parameters calculated to ISC_{II}		
	\overline{Z}	Eag-So	\overline{Z}	Ea _s -S ₀	T_1 min	ISC_{I}	ISC_{II}	$\Delta S^{\#}$	$\Delta H^{\!\#}$	$\Delta G^{\#,c}$
1a	-2.5	75.2	-2.3	62.0	36.6	36.8	38.2	4.0	36.9	35.7
1b	-2.4	63.5	-2.2	55.9	36.6	36.7	37.8	3.4	37.1	35.4
1c	-1.9	75.4	-1.9	64.0	36.9	37.0	38.5	3.8	37.3	36.1
2a	-3.4	48.5	-3.7	48.5	36.0	36.0	36.1	5.9	34.6	32.8
2b	-3.3	53.3	-3.6	49.1	36.1	36.1	36.1	4.9	34.6	33.1
2c	-3.4	70.7	-3.7	66.2	36.2	36.3	36.3	5.8	34.8	33.1

^a Energy values are reported in kcal mol⁻¹, except for $\Delta S^{\#}$ which is reported in cal K^{-1} mol⁻¹, entropy units (e.u.). ^b Values reported in contrast to the E isomer. ^c Values calculated at 65 °C.



Scheme 4 Proposed isomerization reaction pathways: paths a-c through biradical species and paths d-e through a simple twist of the double bond.

the compounds (Scheme 4, paths d,e). This finding allows us to extrapolate the mechanism proposed for 1a to other studied compounds, even for derivatives obtained through changing the functionality of the sulphur atom in the bicyclic counterparts.

As can be seen in Fig. 5 for 2a-c and Fig. S6 (ESI†) for the rest, the T₁ surface presents lower energy than the maximum of S₀, still having a minimum at almost 100° which is very similar to the one obtained for the maximum of So. In addition, when analysing the PES for the ground state (So) and T1 along the $E \rightarrow Z$ torsional pathway, two ISCs (ISC-I and ISC-II) were found. The energy values of these two points are very similar, being slightly more energetic for the simpler derivatives (1a-c), as shown in Table 3. The fact that the biradical channel over single torsion in the ground state is the most plausible, suggesting that thermal isomerization could occur via a triplet state, achieved by an ISC between the So and T1 surfaces, for all the compounds under study, as was demonstrated previously for compound 1a.17 All other relevant parameters can be found

On the other hand, we calculated the theoretical activation entropy $(\Delta S^{\#})$, activation enthalpy $(\Delta H^{\#})$, and activation free energy $(\Delta G^{\#})$ required for thermal reversion $(E \rightarrow Z)$ via the S₀-T₁(ISC-II)-S₀ pathway (Table 3). Based on these studies, a good correlation between the calculated and experimental $\Delta G^{\#}$ was found at the same temperature. As expected, temperatures lower than the boiling point of the solvent (acetonitrile- d_3 , b.p.: 80 °C) render the energy for the thermal reversion.

It is noteworthy that within each family, the larger the crosssection coefficient ($\log \varepsilon$), the greater the percentage of the E isomer in the PSS (Table 2). Additionally, the ISC-II energies of compound 2a-c are lower compared to the corresponding values for 1a-c, which correlate with the higher proportion of the less stable isomer *E*. Therefore, the proportion of isomers in the PSS is given by a combination of the effects produced by these parameters on photoisomerization and thermal reversion, which could raise an explanation for the change in the isomer ratio of both compounds upon irradiation.

In our previous work, fully unconstrained optimizations were recalculated at the CASSCF level (CAS(6/5)/6-31g(d)) of the PES (So and Ti) of 1a in order to shed light on thermal reversion. Nevertheless, the method failed due to the intrinsic lack of the correction for the correlation energy. In the present work, we calculated all barriers for a new set of thioxoimidazolidinone (1b,c) and imidazothiazolone (2a-c) derivatives with the same method and basis set used for 1a.17 Here again, the obtained energy barrier was overcome, in accordance with the experimental results, thus, we conclude that energy correction is crucial in these kinds of calculations.

DNA interaction. In order to evaluate if there is an interaction between dsDNA and some of our derivatives (namely 1a and 2a, which were selected as representative models), their luminescence properties were studied. These compounds are good candidates as fluorescent probes due to their planar structure and the heteroatoms that may form hydrogen bonds.

PCCP Paper

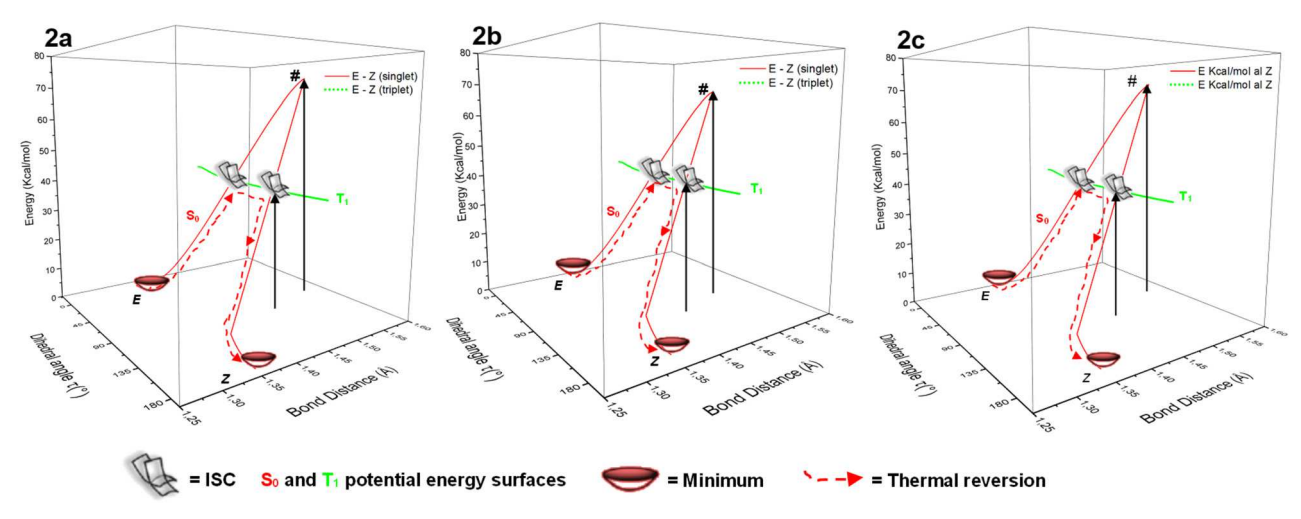


Fig. 5 S₀ and T₁ potential energy surfaces (PES) obtained for compounds 2a-c

It was already studied that there is a DNA interaction with some 5-benzylidene-hydantoin²⁷ and 5-benzylidene-thiohydantoin;¹⁶ however, to the best of our knowledge, there are no studies in the literature with the imidazothiazolones presented in this work.

As explained above, the photoisomerization of these compounds is well established. This process is the main cause of their low emission in solution. However, an enhancement of the emission should be observed if the fluorophore is trapped in a confined environment.²⁸ Considering that $E \rightarrow Z$ isomerization is a thermal controlled process, the reason why all the experiments about dsDNA interactions were performed at 30 °C is because through NMR studies it was observed that only the Z isomer is present at temperatures above 30 °C for all compounds.

The fluorescent profile was examined in the absence and presence of fish dsDNA (0.025%P/P in buffer TE). Solutions of the samples (1a and 2a) were prepared in DMSO reaching a final concentration of 300 µM. Ethidium bromide (EtBr) was employed as a positive control and it was used at a lower concentration of 15 µM due to its self-quenching.

The results are shown in Fig. 6, where the emission of the compounds is compared with and without the presence of dsDNA (after 4 hours of incubation at 30 °C). It can be observed that compound 2a interacts better with dsDNA than the other molecules. When dsDNA is added to a solution of 2a the fluorescence increased up to eightfold. In addition, the emission maxima present a blueshift from 452 nm (free molecule) to 437 nm (molecule-DNA complex). This interaction, though not completely disentangled, could be understood by assuming that 2a retains its planar structure after non-specific binding with DNA, while this could not be the case for 1a. Nevertheless, both chromophores are compounds that possess benzylideneimidazolidin-one moiety which could suggest that both have a similar mode of interaction with dsDNA involving a π - π stacking interaction between the aromatic arylmethylene moiety and the base pairs of dsDNA or through the heteroatoms that may form hydrogen bonds. It seems to be generally accepted that the

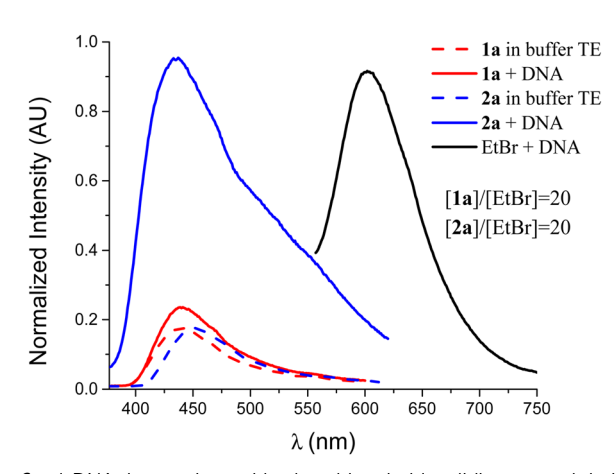


Fig. 6 dsDNA interaction with the thioxoimidazolidinone and imidazothiazolone compounds.

enhanced fluorescence is consistent with the strength of intercalative interaction. In this case, the results are indicating that compound 2a binds more strongly than 1a, penetrating more deeply into, and stacking more strongly with base pairs of dsDNA. This can be rationalized since 2a has a larger planar area and more extended π system than 1a, acquiring a higher rigidity in its interaction within the grooves of dsDNA. The difference in planarity can be observed from the calculated dihedral angles for the styryl moiety for 1a and 2a, which are 21.29° and 0.09° respectively (Fig. S7, page S17 in the ESI†). In turn, as compound 1a would bind more weakly to the dsDNA, it would have a greater conformational freedom allowing the existence of rotamers, which creates additional conformational disorder to that generated by its own prototropic tautomerism.

Regardless of the higher concentration of studied compounds in contrast to EtBr, we believe that compound 2a could perform as a fluorescent probe because its emission appears well within the visible region besides its reduced toxicity. Additionally, its interaction with DNA can lead to a candidature for further trials as anticancer drugs.

PCCP Paper

Conclusion

In this contribution, the synthesis and photoisomerization studies of a family of 5-arylmethylene thioxoimidazolidinones and imidazothiazolones are presented. Kinetics parameters were determined experimentally, and the results denote an enthalpy-entropy compensation effect for the series of reactions under study. Although a major part of molecular switches is based on azobenzenes, the GFP-like chromophores presented in this work could be considered in the design of molecular photoswitches due to their thermal and photochemical stability.

The preliminary investigations about the labelling of dsDNA with thioxoimidazothiazolone 2a are promising. Further investigations are needed to understand the interaction mechanism and fluorescence effects, as well as with different molecular scaffolds.

Author contributions

MSF: investigation, validation, formal analysis (DFT calculations), writing - first draft. EAD: investigation, validation. NMC: investigation, formal analysis (DFT calculations). ENRP: investigation, formal analysis (DFT calculations). LL: investigation, validation. GAA: reviewing and editing. MBP: writing - first draft. NBS: conceptualization, formal analysis, reviewing, and editing. WJP: Conceived and designed the experiments, conceptualization, formal analysis, writing - reviewing, and editing.

Conflicts of interest

There are no conflicts to declare.

Acknowledgements

The authors are grateful for support from the NSF Award (DMR-2103722) and SC EPSCoR GEAR. The work at the Instituto de Investigaciones en Fisicoquímica de Córdoba (INFIQC) was supported by Consejo Nacional de Investigaciones Científicas y Técnicas (CONICET grant number: PIP 11220170100423CO), Fondo para la Investigación Científica y Tecnológica (FONCyT grant number: PICT-2017-1555) and Secretaría de Ciencia y Tecnología (SeCyT-UNC grant number: SeCyT-N°411/18). The NBS acknowledges the support from the NSF Award (DMR-2103722). MSF thanks for the fellowship from Fulbright and CONICET. This work used computational resources from CCAD-UNC (http://ccad.unc.edu.ar/), in particular the Mendieta Cluster, which is part of SNCAD-MinCyT.

References

- 1 M. Zimmer, Green Fluorescent Protein (GFP): Applications, Structure, and Related Photophysical Behavior, Chem. Rev., 2002, 102, 759-782, DOI: 10.1021/cr010142r.
- 2 H. Niwa, S. Inouye, T. Hirano, T. Matsuno, S. Kojima, M. Kubota, M. Ohashi and F. I. Tsuji, Chemical nature of

- the light emitter of the Aequorea green fluorescent protein, Proc. Natl. Acad. Sci. U. S. A., 1996, 93, 13617-13622, DOI: 10.1073/pnas.93.24.13617.
- 3 H. Deng, C. Yu, D. Yan and X. Zhu, Dual-Self-Restricted GFP Chromophore Analogues with Significantly Enhanced Emission, J. Phys. Chem. B, 2020, 124, 871-880, DOI: 10.1021/ acs.jpcb.9b11329.
- 4 M. Ikejiri, H. Kojima, Y. Fugono, A. Fujisaka, Y. Chihara and K. Miyashita, Synthesis and properties of geometrical 4-diarylmethylene analogs of the green fluorescent protein chromophore, Org. Biomol. Chem., 2018, 16, 2397-2401, DOI: 10.1039/C8OB00208H.
- 5 A. Singh, S. Karmakar, I. M. Abraham, D. Rambabu, D. Dave, R. Manjithaya and T. K. Maji, Unraveling the Effect on Luminescent Properties by Postsynthetic Covalent and Noncovalent Grafting of GFP Chromophore Analogues in Nanoscale MOF-808, Inorg. Chem., 2020, 59, 8251-8258, DOI: 10.1021/acs.inorgchem.0c00625.
- 6 E. A. Dolgopolova, T. M. Moore, O. A. Ejegbavwo, P. J. Pellechia, M. D. Smith and N. B. Shustova, A metalorganic framework as a flask: photophysics of confined chromophores with a benzylidene imidazolinone core, Chem. Commun., 2017, 53, 7361-7364, DOI: 10.1039/C7CC02253K.
- 7 R. Saito, M. Hoshi, A. Kato, C. Ishikawa and T. Komatsu, Green fluorescent protein chromophore derivatives as a new class of aldose reductase inhibitors, Eur. J. Med. Chem., 2017, 125, 965-974, DOI: 10.1016/j.ejmech.2016.10.016.
- 8 M.-Y. Wang, Y.-Y. Jin, H.-Y. Wei, L.-S. Zhang, S.-X. Sun, X.-B. Chen, W.-L. Dong, W.-R. Xu, X.-C. Cheng and R.-L. Wang, Synthesis, biological evaluation and 3D-QSAR studies of imidazolidine-2,4-dione derivatives as novel protein tyrosine phosphatase 1B inhibitors, Eur. J. Med. Chem., 2015, 103, 91-104, DOI: 10.1016/j.ejmech.2015.08.037.
- 9 S. Q. Tang, Y. Y. I. Lee, D. S. Packiaraj, H. K. Ho and C. L. L. Chai, Systematic Evaluation of the Metabolism and Toxicity of Thiazolidinone and Imidazolidinone Heterocycles, Chem. Res. Toxicol., 2015, 28, 2019-2033, DOI: 10.1021/acs.chemrestox.5b00247.
- 10 M. S. Faillace, A. P. Silva, A. L. A. B. Leal, L. M. da Costa, H. M. Barreto and W. J. Peláez, Sulfurated and oxygenated imidazoline derivatives: synthesis, antioxidant activity and light-mediated antibacterial activity, ChemMedChem, 2020, 15(10), 851-861, DOI: 10.1002/cmdc.202000048.
- 11 M. S. Faillace, A. L. Alves Borges Leal, F. Araújo de Oliveira Alcântara, J. H. L. Ferreira, J. P. de Siqueira-Júnior, C. E. Sampaio Nogueira, H. M. Barreto and W. J. Peláez, Inhibition of the NorA efflux pump of S. aureus by (Z)-5-(4-Fluorobenzylidene)-Imidazolidines, Bioorg. Med. Chem. Lett., 2021, 31, 127670, DOI: 10.1016/j.bmcl.2020.127670.
- 12 P. D. Halley, C. R. Lucas, E. M. McWilliams, M. J. Webber, R. A. Patton, C. Kural, D. M. Lucas, J. C. Byrd and C. E. Castro, Daunorubicin-Loaded DNA Origami Nanostructures Circumvent Drug-Resistance Mechanisms in a Leukemia Model, Small, 2016, 12, 308-320, DOI: 10.1002/smll.201502118.
- 13 F. Yang, S. S. Teves, C. J. Kemp and S. Henikoff, Doxorubicin, DNA torsion, and chromatin dynamics, Biochim. Biophys. Acta,

- Rev. Cancer, 2014, 1845, 84-89, DOI: 10.1016/j.bbcan.2013. 12,002.
- 14 J. Riedl, P. Ménová, R. Pohl, P. Orság, M. Fojta and M. Hocek, GFP-like Fluorophores as DNA Labels for Studying DNA-Protein Interactions, J. Org. Chem., 2012, 77, 8287-8293, DOI: 10.1021/jo301684b.
- 15 M. Ikejiri, M. Tsuchino, Y. Chihara, T. Yamaguchi, T. Imanishi, S. Obika and K. Miyashita, Design and Concise Synthesis of a Novel Type of Green Fluorescent Protein Chromophore Analogue, Org. Lett., 2012, 14, 4406-4409, DOI: 10.1021/ol301901e.
- 16 A. G. Majouga, A. V. Udina, E. K. Beloglazkina, D. A. Skvortsov, M. I. Zvereva, O. A. Dontsova, N. V. Zyk and N. S. Zefirov, Novel DNA fluorescence probes based on 2thioxo-tetrahydro-4H-imidazol-4-ones: synthetic and biological studies, Tetrahedron Lett., 2012, 53, 51-53, DOI: 10.1016/j.tetlet.2011.10.118.
- 17 A. J. Pepino, M. A. Burgos Paci, W. J. Peláez and G. A. Argüello, An experimental and theoretical study of the photoisomerization and thermal reversion on 5-arylmethylene-2-thioxoimidazolidin-4-one, Phys. Chem. Chem. Phys., 2015, 17, 12927-12934, DOI: 10.1039/C4CP04748F.
- 18 A. J. Pepino, W. J. Peláez, M. S. Faillace, N. M. Ceballos, E. L. Moyano and G. A. Argüello, (S)-5-Benzyl- and 5-benzylideneimidazo-4-one derivatives synthesized and studied for an understanding of their thermal reactivity, RSC Adv., 2014, 4, 60092-60101, DOI: 10.1039/C4RA11046C.
- 19 M. J. Frisch, G. W. Trucks, H. B. Schlegel, G. E. Scuseria, M. A. Robb, J. R. Cheeseman, G. Scalmani, V. Barone, B. Mennucci and G. A. Petersson, Gaussian 09, revision E. 01 Inc., Wallingford CT, 2009.
- 20 E. G. Jayasree and S. Sreedevi, A DFT study on protic solvent assisted tautomerization of heterocyclic thiocarbonyls, Chem. Phys., 2020, 530, 110650, DOI: 10.1016/j.chemphys. 2019.110650.
- 21 S. Bagheri and H. Roohi, Proton-Transfer Mechanism in 2-Thioxoimidazolidin-4-one: A Competition between Keto/Enol

- and Thione/Thiol Tautomerism Reactions, BCSJ, 2009, 82, 446-452, DOI: 10.1246/bcsj.82.446.
- 22 S.-F. Tan, K.-P. Ang and G.-F. How, Thermal equilibration of Z- and E-isomers of 5-arylmethylenehydantoins. Evidence for non-bonded aromatic π ···methyl attractions, *I. Chem.* Soc., Perkin Trans. 2, 1988, 2045-2049, DOI: 10.1039/ P29880002045.
- 23 S.-F. Tan, K.-P. Ang and G.-F. How, Z/E, photoisomerization of 5-arylmethylenehydantoins and 5-pyridylmethylenehydantoins, J. Phys. Org. Chem., 1991, 4, 707-713, DOI: 10.1002/poc.610041202.
- 24 J. Dong, F. Abulwerdi, A. Baldridge, J. Kowalik, K. M. Solntsev and L. M. Tolbert, Isomerization in Fluorescent Protein Chromophores Involves Addition/Elimination, I. Am. Chem. Soc., 2008, 130, 14096–14098, DOI: 10.1021/ ja803416h.
- 25 J.-J. Xu, R. Sung and K. Sung, S₁/S₀ Potential Energy Surfaces Experience Different Types of Restricted Rotation: Restricted Z/E Photoisomerization and E/Z Thermoisomerization by an Out-of-Plane Benzyl Group or In-Plane m-Pyridinium Group?, J. Phys. Chem. A, 2019, 123, 4708-4716, DOI: 10.1021/acs.jpca.9b02924.
- 26 L. Liu and Q.-X. Guo, Isokinetic Relationship, Isoequilibrium Relationship, and Enthalpy-Entropy Compensation, Chem. Rev., 2001, 101, 673-696, DOI: 10.1021/cr990416z.
- 27 A. Shah, E. Nosheen, S. Munir, A. Badshah, R. Qureshi, Z. Rehman, N. Muhammad and H. Hussain, Characterization and DNA binding studies of unexplored imidazolidines by electronic absorption spectroscopy and cyclic voltammetry, J. Photochem. Photobiol., B, 2013, 120, 90-97, DOI: 10.1016/j.jphotobiol.2012.12.015.
- 28 A. Fürstenberg, M. D. Julliard, T. G. Deligeorgiev, N. I. Gadjev, A. A. Vasilev and E. Vauthey, Ultrafast Excited-State Dynamics of DNA Fluorescent Intercalators: New Insight into the Fluorescence Enhancement Mechanism, J. Am. Chem. Soc., 2006, 128, 7661-7669, DOI: 10.1021/ ja0609001.